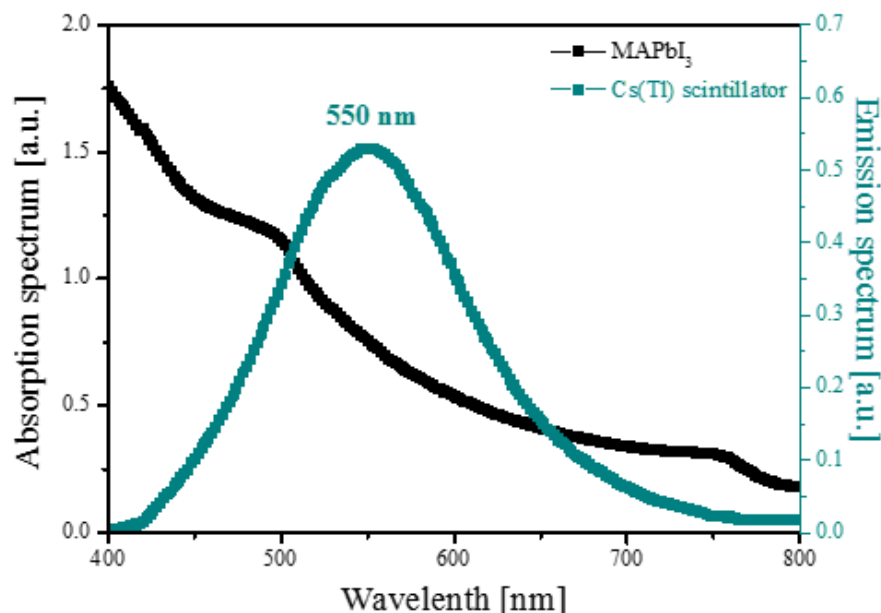


**SUPPLEMENTARY INFORMATION**  
**Characteristics of a hybrid detector combined with a perovskite active layer for indirect X-ray detection**

Hailiang Liu, Jehoon Lee and Jungwon Kang\*

Department of Electronic and Electrical Engineering, Dankook University, Gyeonggi-do 16890, Korea;  
 liuhailiang107@gmail.com (H.L.); usyj0512@gmail.com (J.L.); jkang@dankook.ac.kr (J.K.)

\* Correspondence: jkang@dankook.ac.kr; Tel.: +82-31-8005-3624 (J.K)



**Figure S1.** Absorption spectrum of the optimized perovskite layer with a thickness of 192 nm annealed at 100°C and the emission spectrum of the CsI(Tl) scintillator.

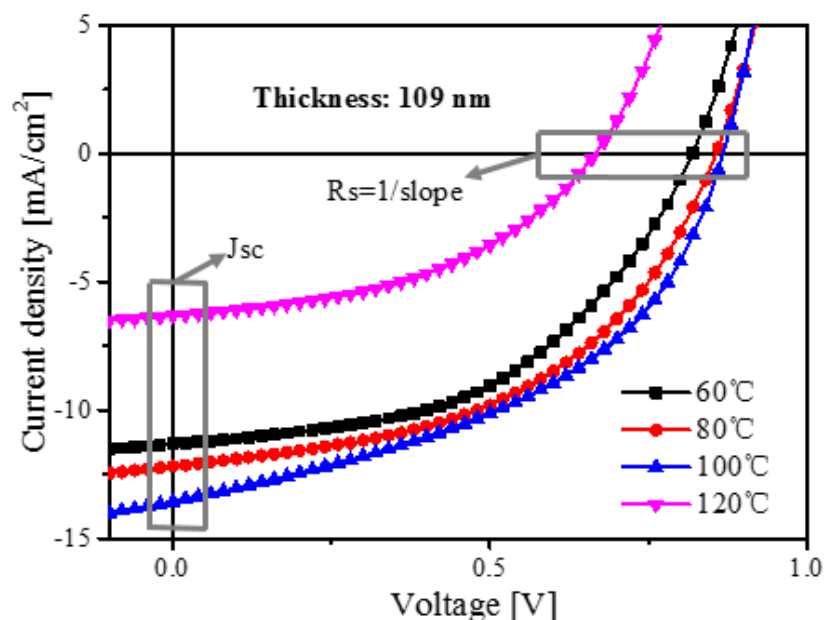


**Figure S2.** Current density-voltage (J-V) characteristics of the detectors based on 109-nm thick  $\text{MAPbI}_3$  under different annealing temperatures.

**Table S1.**  $J_{SC}$ ,  $R_s$ , CCD and Sensitivity of the detectors based on 109-nm thick  $\text{MAPbI}_3$  under different annealing temperatures.

Temperature [°C]	$J_{SC}$ [mA/cm <sup>2</sup> ]	$R_s$ [Ω]	CCD [μA/cm <sup>2</sup> ]	Sensitivity [mA/Gy·cm <sup>2</sup> ]
60	$11.31 \pm 0.67$	$301.13 \pm 3.7$	$6.62 \pm 0.12$	$1.68 \pm 0.05$
80	$12.18 \pm 0.65$	$292.19 \pm 3.7$	$7.79 \pm 0.13$	$2.01 \pm 0.06$
100	$13.56 \pm 0.63$	$282.11 \pm 3.9$	$8.46 \pm 0.14$	$2.11 \pm 0.06$
120	$6.32 \pm 0.71$	$381.23 \pm 4.0$	$5.47 \pm 0.14$	$1.35 \pm 0.07$

The difference value between positive and negative in all tables represent the standard deviation based on 10 devices per condition.

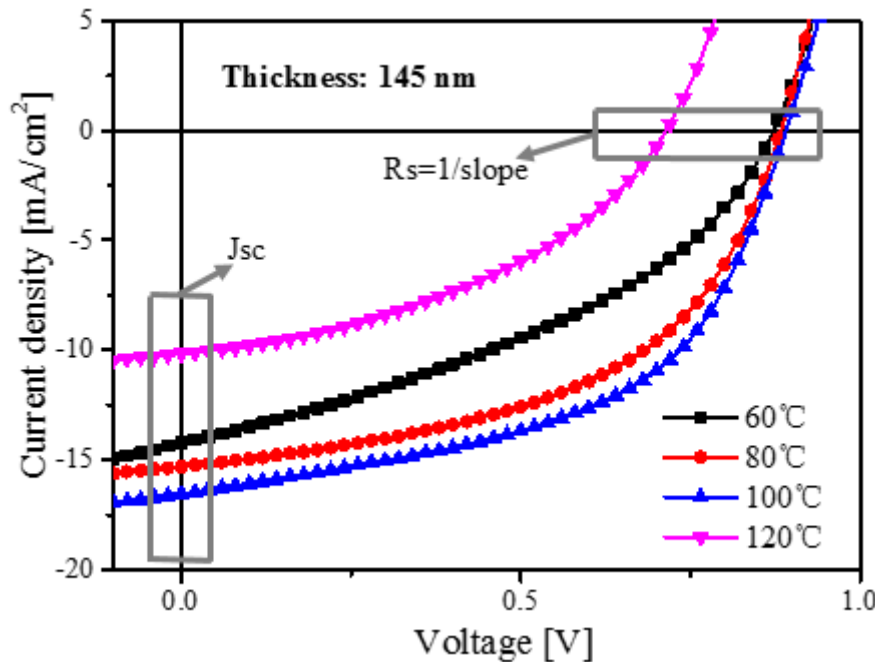


**Figure S3.** Current density-voltage (J-V) characteristics of the detectors based on 145-nm thick  $\text{MAPbI}_3$  under different annealing temperatures.

**Table S2.**  $J_{SC}$ ,  $R_s$ , CCD and Sensitivity of the detectors based on 145-nm thick  $\text{MAPbI}_3$  under different annealing temperatures.

Temperature [°C]	$J_{SC}$ [mA/cm <sup>2</sup> ]	$R_s$ [Ω]	CCD [μA/cm <sup>2</sup> ]	Sensitivity [mA/Gy·cm <sup>2</sup> ]
60	$14.23 \pm 0.64$	$261.73 \pm 3.8$	$8.32 \pm 0.11$	$2.14 \pm 0.06$
80	$15.31 \pm 0.62$	$258.13 \pm 3.7$	$8.47 \pm 0.12$	$2.18 \pm 0.05$
100	$16.54 \pm 0.61$	$198.36 \pm 3.8$	$9.32 \pm 0.13$	$2.33 \pm 0.07$
120	$10.17 \pm 0.68$	$316.54 \pm 3.9$	$6.22 \pm 0.14$	$1.57 \pm 0.08$

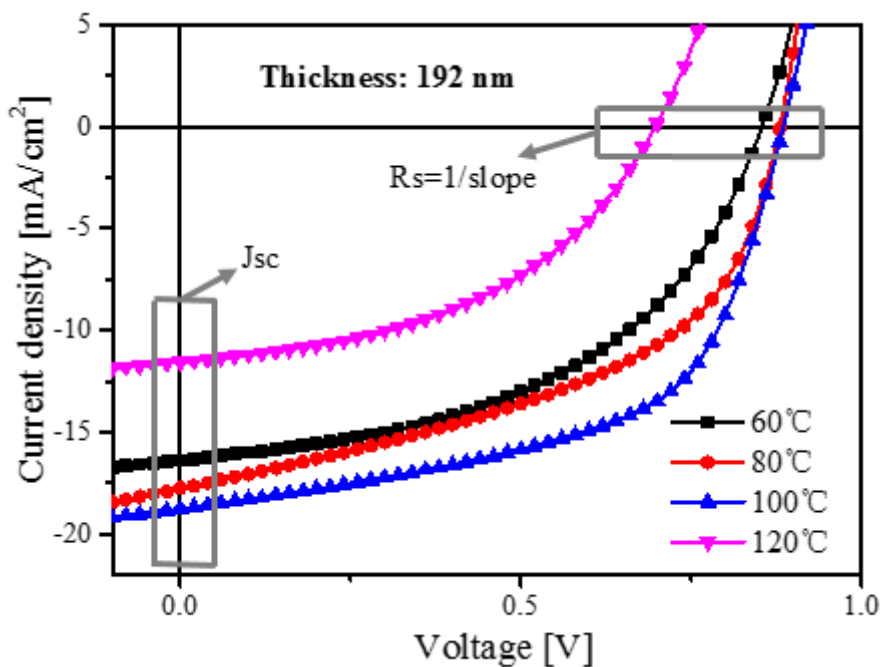


**Figure S4.** Current density-voltage (J-V) characteristics of the detectors based on 192-nm thick MAPbI<sub>3</sub> under different annealing temperatures.

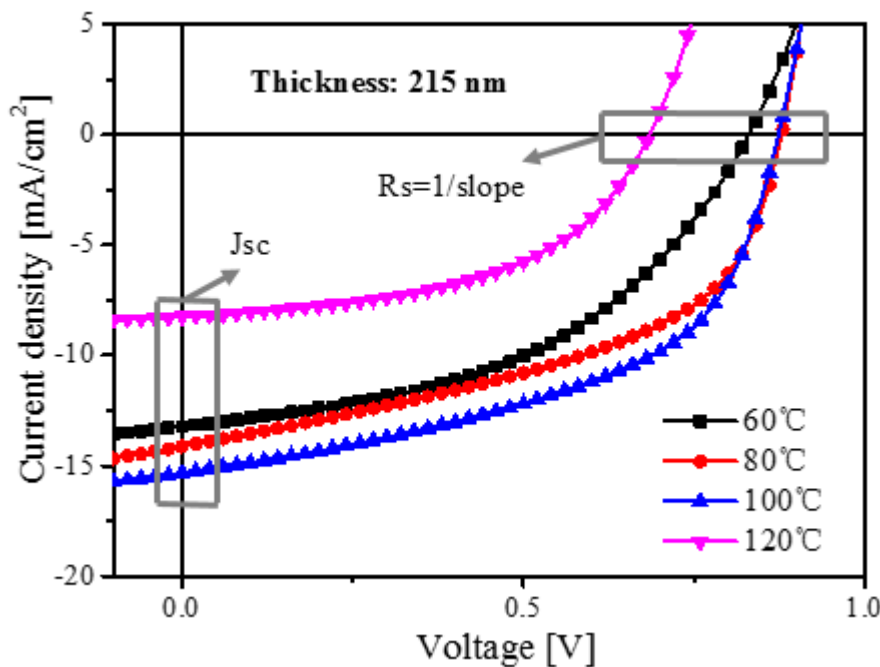


**Figure S5.** Current density-voltage (J-V) characteristics of the detectors based on 215-nm thick MAPbI<sub>3</sub> under different annealing temperatures.

**Table S3.**  $J_{SC}$ ,  $R_S$ , CCD and Sensitivity of the detectors based on 215-nm thick  $\text{MAPbI}_3$  under different annealing temperatures.

Temperature [°C]	$J_{SC}$ [mA/cm <sup>2</sup> ]	$R_S$ [Ω]	CCD [μA/cm <sup>2</sup> ]	Sensitivity [mA/Gy·cm <sup>2</sup> ]
60	$13.23 \pm 0.66$	$274.78 \pm 3.7$	$8.06 \pm 0.13$	$2.06 \pm 0.08$
80	$14.13 \pm 0.64$	$268.32 \pm 3.8$	$8.35 \pm 0.12$	$2.13 \pm 0.09$
100	$15.32 \pm 0.62$	$256.09 \pm 3.8$	$8.76 \pm 0.13$	$2.19 \pm 0.07$
120	$8.26 \pm 0.69$	$341.78 \pm 3.9$	$5.93 \pm 0.14$	$1.47 \pm 0.10$



© 2020 by the authors. Licensee MDPI, Basel, Switzerland. This article is an open access article distributed under the terms and conditions of the Creative Commons Attribution (CC BY) license (<http://creativecommons.org/licenses/by/4.0/>).